This is a preprint, the final version is subject to change, of the American Mineralogist (MSA)
Cite as Authors (Year) Title. American Mineralogist, in press.
DOI: https://doi.org/10.2138/am-2018-6399

Sodium amphibole in the post-glaucophane high-pressure domain: the role of eckermannite *Revision 1*

Harriet Howe[1], Alison R. Pawley[1], Mark D. Welch[2]

[1]School of Earth and Environmental Sciences, University of Manchester, Manchester M13 9PL, United Kingdom.

[2]Department of Earth Sciences, Natural History Museum, London SW7 5BD, United Kingdom.

Abstract

An amphibole close to eckermannite in composition, ideally $Na_3Mg_4AlSi_8O_{22}(OH)_2$, was encountered in experiments on a bulk composition close to that of glaucophane at 6.2 GPa, ~550–650 ºC. The synthetic amphibole has an average composition corresponding to $^{A}Na_{0.96}\ ^{B}(Na_{1.80}Mg_{0.20})\ ^{C}(Mg_4Al)\ ^{T}(Si_{7.85}Al_{0.15})O_{22}(OH)_2$. This composition is displaced from that of endmember eckermannite by exchange vectors $+0.15\ ^{B}Mg\ ^{T}Al\ ^{B}Na_{-1}\ ^{T}Si_{-1}$ and $+0.05\ ^{A}o\ ^{B}Mg\ ^{A}Na_{-1}\ ^{B}Na_{-1}$ (o = vacant site). In terms of endmembers, it corresponds to 80% eckermannite + 15% Mg-katophorite, $Na(NaMg)(Mg_4Al)(Si_7Al)O_{22}(OH)_2$, + 5% Mg-winchite, $(NaMg)(Mg_4Al)Si_8O_{22}(OH)_2$, and as such is essentially binary. The absence of a glaucophane component implies that the stability of sodium amphibole at very high pressures (>4 GPa) involves eckermannitic rather than glaucophanic compositions. The stabilization of the eckermannite-pyrope tie line allows this highly Na-rich amphibole to occur even in bulk compositions that are not particularly Na-rich. In blueschist facies metabasites, it is possible that eckermannite forms by the reaction 9 jadeite + 7 talc $\rightarrow$ 3 eckermannite + 3 pyrope + 13 coesite + 4 H_2O, above the stability limit of glaucophane that is defined by the reaction glaucophane $\rightarrow$ 2 jadeite + talc.

Key words: glaucophane, eckermannite, high pressure, blueschist, subduction

Introduction

Eckermannite is a rare member of the sodium amphibole group, having an ideal formula $Na_3Mg_4AlSi_8O_{22}(OH)_2$, with Na filling the A and M(4) sites. The only occurrence reported in the literature is from the Jade Mine Tract, Myanmar, a serpentinite mélange containing tectonic blocks and veins of jadeitite (Oberti et al., 2015). Eckermannite from this locality is interpreted as having a metasomatic origin from interaction of sodium-rich fluids with serpentinite, while the presence of jadeite indicates high-pressure, low-temperature conditions, estimated at between 1.0 and 1.5 GPa, and 300 °C to 450 °C (Shi et al., 2012). All previously described eckermannitic amphiboles are associated with alkaline igneous rocks such as syenites and carbonatites. However, these amphiboles are enriched in Fe, Li and/or F, and thus the former holotype from the Norra Kärr nepheline syenite, Sweden, has been reclassified as fluoro-leakeite, and characterization of the eckermannite from the Jade Mine Tract has resulted in a new holotype (Oberti et al., 2015).

The apparent restriction of eckermannite to high-pressure rocks indicates that it is a potential blueschist-facies sodium amphibole. However, its stability and phase relations are unknown. Previous attempts to synthesize eckermannite at low pressures have not been successful: Raudsepp et al. (1991) obtained a 98% amphibole product at 0.2 GPa and 817 °C; however, the amphibole was not eckermannite, but an A-site empty amphibole inferred to be a solid solution between $NaMg_5AlSi_8O_{22}(OH)_2$ and glaucophane.

Previous high-pressure experimental studies of the phase relations of sodium amphiboles have, unsurprisingly, focused on glaucophane, $Na_2Mg_3Al_2Si_8O_{22}(OH)_2$, the most common blueschist-facies amphibole. Consistent results have been obtained from synthesis experiments on the bulk composition of glaucophane (Koons, 1982; Tropper et al., 2000), its fluorine analogue $Na_2Mg_3Al_2Si_8O_{22}F_2$ (Welch and Graham, 1992) and the closely related amphibole nyböite

$Na_3Mg_3Al_2Si_7AlO_{22}(OH)_2$ (Pawley, 1992). All studies produced an essentially binary glaucophane-nyböite amphibole that is nyböite-rich at P <2 GPa and evolves toward glaucophane at 2.5–3 GPa (600–800 °C), primarily by the coupled substitution $^{A}o\ ^{T}Si\ ^{A}Na_{-1}\ ^{T}Al_{-1}$ (o = vacant A site).

The high-pressure limit of glaucophane stability is governed by the reaction glaucophane → jadeite + talc. The position of this reaction has been determined in reversal experiments by Corona et al. (2013) using a synthetic amphibole approaching endmember glaucophane in composition: $^{A}Na_{0.08}\ ^{B}(Na_{1.83}Mg_{0.17})\ ^{C}(Mg_{3.12}Al_{1.88})\ ^{T}(Si_{7.89}Al_{0.11})O_{22}(OH)_2$. The linear reaction boundary was located at 2.6 GPa/600 °C to 3.1 GPa/700 °C. Data on the stability of sodium amphibole above this reaction are scarce. Here we report the synthesis of eckermannite at 6.2 GPa and 550–650 °C, and show that it could be a significant post-glaucophane phase in subducted metabasites, giving it the potential to store Na, water and trace elements in deeply subducted oceanic crust.

Experimental

Synthesis experiments

Compositions of phases relevant to this study are shown in Figure 1. The starting material for the experiments was a mixture of synthetic brucite, $Mg(OH)_2$, ground silica glass and a previously-prepared gel of jadeite composition, with the bulk composition $Na_{2.1}Mg_{4.9}Al_{2.1}Si_{6.95}O_{23}$ + excess H_2O. All experiments were run in a multi-anvil apparatus, using an 18/12 sample assembly (18-mm octahedron edge length, 12-mm truncated edge lengths on the tungsten carbide cubes). The first experiment was intended to investigate the incorporation of Na and Al into the 10-Å phase. It was run at 6.2 GPa, 510–620 °C (the large temperature uncertainty was due to a broken thermocouple), 77 h. However, no 10-Å phase was produced, and instead amphibole was

formed, together with jadeite + coesite + pyrope. Another three experiments were then run for further exploration of amphibole stability. They were also run at 6.2 GPa, with temperatures in the range 570–690 °C (thermocouple breakages occurred in another two of these experiments), and run durations between 48 and 100 h. Run products were identified using powder XRD. All runs produced amphibole ± jadeite ± pyrope ± coesite ± sheet silicate. Water was present in excess in all runs. Amphibole was most abundant in Experiment 2, where it coexisted with pyrope + sheet silicate + coesite.

The amphibole crystals from all experiments are acicular, with diameters <0.01 mm and lengths of up to 0.15 mm (Fig. 2a). High-resolution transmission-electron microscopy (HRTEM) shows no evidence of any visible defects in the crystals (Fig. 2b). The compositions of amphibole crystals from Experiment 2 were determined by electron-microprobe analysis (EMPA) using a Cameca SX100 Electron Microprobe, operated at 15 keV, 20 nA, and with the following standards: fayalite (Si), periclase (Mg), jadeite (Na), corundum (Al). The average of ten electron-microprobe spot analyses is (wt%) 58.83 SiO_2, 7.23 Al_2O_3, 21.02 MgO, 10.62 Na_2O, which corresponds to the structural formula $^{A}Na_{0.96}\ ^{B}(Na_{1.80}Mg_{0.20})\ ^{C}(Mg_4Al)\ ^{T}(Si_{7.85}Al_{0.15})O_{22}(OH)_2$. In terms of amphibole endmember components, this formula is 80% eckermannite, 15% Mg-katophorite, 5% Mg-winchite. The identification of the last two components is made with reference to the most recent nomenclature of Hawthorne et al. (2012). We point out that these two amphibole endmembers have no natural counterparts, and so for ease of discussion we have named them to be consistent with Hawthorne et al. (2012) for katophorite $^{A}Na\ ^{B}(NaCa)\ ^{C}(Mg_4Al)\ ^{T}Si_7AlO_{22}(OH)_2$, and winchite $^{A}o\ ^{B}(NaCa)\ ^{C}(Mg_4Al)\ ^{T}Si_8O_{22}(OH)_2$, recognising that the "Mg-" identifier denotes Mg replacing Ca at the M(4) site.

The sheet silicate was identified as aspidolite, $NaMg_3AlSi_3O_{10}(OH)_2$, from its distinctive hydration state at room temperature (Carman, 1974). By analogy with previous experiments in

which aspidolite was formed (Pawley, 1992), the sheet silicate may show solid solution toward preiswerkite, $NaMg_2Al_3Si_2O_{10}(OH)_2$.

X-ray diffraction

Numerous crystals of synthetic eckermannite were screened by single-crystal X-ray diffraction (SCXRD) to check diffraction quality using an Xcalibur four-circle diffractometer equipped with an EoS area detector and operated at 45 kV, 40mA with Mo$K\alpha$ radiation (λ = 0.71073 Å). However, all crystals were very weakly diffracting due to their extreme thinness (0.005 mm) and the presence of only weak X-ray scatterers (O, Na, Mg, Al, Si). A full data collection to 27.5 °θ using a frame-time of 240 s, was attempted on the best crystal, but the reflection merging was very poor (R_{int} = 0.26), again due to the weakness of the reflections (R_σ = 0.414) and extremely acicular nature of the crystal. However, sufficient stronger reflections having $I > 7\sigma$ (I) allowed derivation of precise unit-cell parameters (monoclinic, space group $C2/m$): a 9.726(4) Å, b 17.757(6) Å, c 5.278(2) Å, β 103.58(3)°, V 886.0(6) Å^3.

A quasi-powder pattern for an aggregate of eckermannite crystals from Experiment 2 mounted on a 0.01 mm diameter carbon-fibre support was collected using a Rigaku Oxford Diffraction RAPIDII curved-imaging-plate diffractometer with graphite-monochromated Cu$K\alpha$ radiation (45 kV, 20 mA). A Gandolfi-type randomized movement was achieved by rotation around the φ and ω axes. The General Structure Analysis System GSAS (Toby and Von Dreele, 2013) was used for Rietveld refinement. The starting structural model used was taken from Oberti et al. (2015) for eckermannite from Myanmar with the structural formula $^{A}(Na_{0.87}K_{0.06})_{\Sigma=0.93}$ $^{B}(Na_{1.89}Ca_{0.11})_{\Sigma=2.00}$ $^{C}(Mg_{3.87}Fe^{2+}_{0.09}Mn_{0.01}Fe^{3+}_{0.38}Al_{0.62})_{\Sigma=4.97}$ $^{T}Si_{8.00}O_{22}$ $^{W}(F_{0.03}OH_{1.97})$. Unit-cell parameters were refined along with the coefficients of a cosine series to model background and Gaussian and Lorentzian lineshape parameters. Preferred orientation was also refined, but found to

be negligible. An attempt to refine atom coordinates and isotropic atom-displacement parameters was successful for some sites, but failed to converge for most. Consequently, atom coordinates and atom-displacement parameters were not refined, but fixed at the values reported by Oberti et al. (2015). The refined unit-cell parameters are in close agreement with those obtained by SCXRD: *a* 9.7278(4) Å, *b* 17.7431(8) Å, *c* 5.2806(2) Å, β 103.541(3)°, *V* 886.10(7) Å^3. Final agreement indices at convergence are R_p = 0.031 and wR_p = 0.043. The fit of the refined pattern is shown in Figure 3.

Raman spectroscopy

The unpolarised Raman spectrum of a single crystal of eckermannite is shown in Figure 4. It comprises an intense peak with a Raman shift of 3729 cm^{-1} and a very minor peak at 3629 cm^{-1}. The 3729 cm^{-1} peak is characteristic of OH associated with an A site occupied by Na and associated with a single local arrangement Mg(1)Mg(1)Mg(3)-OH…^{A}Na (Della Ventura et al. 1997). The separation by 100 cm^{-1} between the two peaks is more than the difference between A-site full and A-site empty local arrangements (usually ~60 cm^{-1}) and suggests contamination by minor sheet silicate (preiswerkite has its main peak at 3628 cm^{-1}, Tlili et al., 1989). The absence of any other OH peaks indicates that the M(1,3) sites are occupied only by Mg and requires that Al is fully ordered at M(2). As such, this spectrum is consistent with the average formula determined by EMPA.

Discussion

We have shown that sodium amphibole coexisting with jadeite, pyrope and coesite at 6.2 GPa and 550–650 °C is highly eckermannitic (80 mol%). The bulk composition used allows for ternary or higher-order solid solution in amphibole. However, we find that the amphibole has an

145 essentially binary *ek–mk* composition. While synthesis experiments do not, of course, demonstrate
146 thermodynamic stability, previous synthesis studies (Koons, 1992; Welch and Graham, 1992;
147 Pawley, 1992; Tropper et al., 2000; Corona and Jenkins, 2007) show convincing systematic trends
148 in amphibole composition as a function of *P* and *T*. It seems reasonable, therefore, to infer that
149 eckermannite-rich amphibole, as encountered in this study, is likely to be stable at 6.2 GPa, 600
150 °C, rather than being a metastable product of the synthesis method.

151 The range of assemblages produced in our experiments probably reflects the nominal bulk
152 composition lying on both the eckermannite–pyrope–coesite and jadeite–aspidolite–coesite joins
153 (Fig. 1), such that small variations in bulk composition and temperature both between experiments
154 and, possibly, within a single experiment, resulted in varying proportions of eckermannite and
155 other phases.

156 Our synthesis pressure is 3 GPa higher than the upper baric limit of glaucophane stability
157 of about 3.2 GPa at 700 °C (Corona et al., 2013). The fact that our sample was synthesized from a
158 bulk composition not far from that of endmember glaucophane raises the question as to why
159 eckermannite has not been synthesized in previous studies of glaucophanic amphiboles. The
160 answer may lie in the bulk compositions used previously, all of which had Na:Al = 1:1. In most
161 cases, the amphiboles had compositions with a Na:Al ratio deviating very little from 1:1, and
162 coexisted with quartz, jadeite and either talc or aspidolite, also with Na:Al = 1:1, indicating that
163 the amphibole composition was buffered onto the jadeite-talc-quartz plane (Fig. 1). The only
164 amphiboles to show a significant eckermannite component were synthesized from a silica-
165 undersaturated bulk composition (Pawley, 1992), for which the sheet silicate showed solid
166 solution toward aspidolite and preiswerkite. The preiswerkite component allowed the amphibole
167 composition to move off the Na:Al = 1 plane. The maximum eckermannite content in those
168 amphiboles was 0.45 *apfu*. Therefore, we suggest that at pressures relevant to glaucophane

169 stability, a bulk composition with high Na:Al would be required to synthesize an amphibole
170 approaching endmember eckermannite. Similarly, in Nature eckermannite has so far only been
171 found in rocks of unusually Na-rich compositions.

172 Our synthesis of eckermannite at 6.2 GPa from a bulk composition with Na:Al = 1:1,
173 shows that at this pressure, the amphibole composition is no longer buffered onto the jadeite-talc-
174 quartz/coesite plane, even for silica-saturated compositions (most of our run products coexist with
175 coesite). It is evident that the stabilization of the eckermannite-pyrope tie line at high pressure
176 (Fig. 1) is key to its synthesis in a bulk composition with Na:Al = 1, as pyrope is Al-rich and Na-
177 free.

178 The high-pressure trend of increasing Na and decreasing Al that occurs from glaucophane
179 to eckermannite is similar to that observed in recent experimental studies on sodium-rich calcium
180 amphiboles. In experiments simulating metasomatism of the mantle wedge by fluids derived by
181 partial melting of subducted sediment, Pirard and Hermann (2015) produced amphiboles close in
182 composition to the sodium-calcium amphibole katophorite, $Na_2CaMg_4AlSi_7AlO_{22}(OH)_2$, at
183 pressures of 2.5–4.5 GPa, with amphibole breaking down at 950–1000 °C at 4.5 GPa. Amphibole
184 compositions showed an increase in Na/Ca toward nyböite with pressure. Mandler and Grove
185 (2016) also observed increasing Na/Ca in amphiboles with pressure, in experiments at 2–4 GPa,
186 950–1100 °C on mantle compositions modified by the addition of 1 % of a metasomatic Na-rich
187 component, which produced pargasitic amphiboles. They also observed a decrease in Al with
188 increasing pressure. Both of these studies produced garnet in higher-pressure experiments (>2
189 GPa), indicating that as the Al content of amphibole decreases with increasing pressure, garnet
190 becomes the main aluminous phase.

191 These recent studies show that Na-rich amphiboles can be synthesized at pressures up to at
192 least 4.5 GPa. Our study takes their stability limit to at least 6 GPa. Mandler and Grove (2016)

point out that high Na/Ca is associated with reduced thermal stability of amphibole, and so eckermannite is likely not to be stable at the high temperatures investigated by Pirard and Hermann (2015) and Mandler and Grove (2016), where katophorite is likely to be the stable amphibole.

An important consequence of the high Na:Al ratio of eckermannite is that it cannot be decomposed into charge-neutral pyroxene and sheet-silicate components, as there are no pyroxenes or sheet silicates in the NMASH system with Na:Al >1. For example, polysomatic decomposition of the eckermannite structure leads to $[Na_2MgAlSi_4O_{12}]^{-1}$ ("pyroxene") and $[NaMg_3Si_4O_{10}(OH)_2]^{+1}$ ("sheet silicate") modules. Analogously, polysomatic decomposition of Al-free K-richterite, $KNaCaMg_5Si_8O_{22}(OH)_2$, would result in $[NaCaMg_2Si_4O_{12}]^{-1}$ ("pyroxene") and $[KMg_3Si_4O_{10}(OH)_2]^{+1}$ ("sheet silicate") modules. K-richterite has the highest reported baric stability of any amphibole, having been synthesized at P >14 GPa at 1000 °C (Trønnes, 2002). A direct consequence of the implied production of energetically unstable charged structure modules is that the usual pressure-stability limit of amphibole defined by the amphibole = pyroxene + sheet-silicate/talc reaction does not occur for K-richterite and eckermannite, and this may be the reason for their exceptionally high baric stabilities.

An alternative polysomatic decomposition reaction for eckermannite can be conceived that involves the triple-chain silicate $Na_2Mg_4Si_6O_{16}(OH)_2$ (Tateyama et al. 1978; Maresch et al. 2013) and jadeite: $Na_3Mg_4AlSi_8O_{22}(OH)_2 \rightarrow NaAlSi_2O_6 + Na_2Mg_4Si_6O_{16}(OH)_2$. In this case, no charged entities are involved. However, triple-chain silicates have relatively low baric stabilities (<1 GPa) compared with amphiboles, and with increasing pressure and temperature decompose to form unusual OH-rich amphiboles having more than 2 OH *pfu* (Witte, 1975; Maresch et al. 2013). For example, the maximum thermal stability of $Na_2Mg_4Si_6O_{16}(OH)_2$ is ~530 °C at 0.2 GPa; at 1 GPa

the limit is 400 °C. Consequently, the decomposition of eckermannite to jadeite and $Na_2Mg_4Si_6O_{16}(OH)_2$ triple-chain silicate is not expected.

Implications

This study is the first to show that eckermannitic amphibole is the likely stable sodium amphibole that succeeds glaucophane in prograde metabasites in the high-*P*/low-*T* domain. As such, it represents an important extension of the baric stability of sodium amphibole. The experiments reported here suggest that eckermannite could be produced by the reaction 9 jadeite + 7 talc $\rightarrow$ 3 eckermannite + 3 pyrope + 13 coesite + 4 H_2O, with the reactants being available from the decomposition of glaucophanic amphibole.

Previous experimental studies of glaucophane and related amphiboles in the presence of quartz/coesite show that at $P \leq 3.5$ GPa, all amphiboles have Na:Al = 1:1 (*gp*, *ny*, *mk*). The present study indicates that at higher pressures, this ratio is expected to change with stabilization of the eckermannite–pyrope tie line, so that Na and Al are partitioned differently between minerals in the post-glaucophane regime of blueschists, with amphibole becoming increasingly important as a host for Na. We propose that the formation of eckermannite at high pressure does not require additional Na enrichment of the host rock, simply the presence of jadeite and talc formed by the decomposition of glaucophane. Consequently, eckermannite is to be expected in metabasites in the post-glaucophane high-*P* regime.

Acknowledgments

This work was supported by a Natural Environment Research Council PhD studentship to Harriet Howe. We thank Heath Bagshaw, Jonathan Fellowes and John Waters for technical assistance and

advice in the analytical labs in Manchester. Reviewers Frank Hawthorne and David Jenkins are thanked for their helpful comments on the manuscript.

References

Carman, J.H. (1974) Synthetic sodium phlogopite and its two hydrates: stabilities, properties, and mineralogic implications. American Mineralogist, 59, 261-273.

Corona, J.C., and Jenkins, D.M. (2007) An experimental investigation of the reaction: glaucophane + 2 quartz = 2 albite + talc. European Journal of Mineralogy, 19, 147-158.

Corona, J.C., Jenkins, D.M., and Holland, T.J.B. (2013) Constraints on the upper pressure stability of blueschist facies metamorphism along the reaction: glaucophane = talc + 2 jadeite in the Na_2O-MgO-Al_2O_3-SiO_2-H_2O system. American Journal of Science, 313, 967-995.

Della Ventura, G., Robert, J-L., Hawthorne, F.C., and Welch, M.D. (1997) Site occupancies in synthetic monoclinic amphiboles: Rietveld refinement and infrared spectroscopy of (nickel, magnesium, cobalt)- richterite. American Mineralogist, 82, 291-301.

Hawthorne, F.C., Oberti, R., Harlow, G.E., Maresch, W.V., Martin, R.F., Schumacher, J.C., and Welch, M.D. (2012) Nomenclature of the amphibole supergroup. American Mineralogist, 97, 2031-2048.

Koons, P.O. (1982) An experimental investigation of the behavior of amphibole in the system Na_2O-MgO-$A1_2O_3$-SiO_2-H_2O at high pressures. Contributions to Mineralogy and Petrology, 79, 258-267.

Mandler, B.E., and Grove, T.L. (2016) Controls on the stability and composition of amphibole in the Earth's mantle. Contributions to Mineralogy and Petrology, 171, 68-77.

Maresch, W.V., Welch, M.D., Gottschalk, M., Ruthmann, W., Czank, M., and Ashbrook, S.E. (2009) Synthetic amphiboles and triple-chain silicates in the system Na_2O-MgO-SiO_2-H_2O:

phase characterization, compositional relations and excess H. Mineralogical Magazine, 73, 957-996.

Oberti, R., Boiocchi, M., Hawthorne, F.C., Ball, N.A., and Harlow, G.E. (2015) Eckermannite revised: The new holotype from the Jade Mine Tract, Myanmar - crystal structure, mineral data, and hints on the reasons for the rarity of eckermannite. American Mineralogist, 100, 909–914.

Pawley, A.R. (1992) Experimental study of the compositions and stabilities of synthetic nyböite and nyböite-glaucophane amphiboles. European Journal of Mineralogy, 4, 171-192.

Pirard, C., and Hermann, J. (2015) Experimentally determined stability of alkali amphibole in metasomatised dunite at sub-arc pressures. Contributions to Mineralogy and Petrology, 169, 1-26.

Raudsepp, M., Turnock, A.C., and Hawthorne, F.C. (1991) Amphibole synthesis at low pressure: what grows and what doesn't. European Journal of Mineralogy, 3, 983-1004.

Shi, G., Harlow, G.E., Wang, J., Wang, J., Ng, E., Wang, X., Cao, S., and Cui, W. (2012) Mineralogy of jadeitite and related rocks from Myanmar: a review with new data. European Journal of Mineralogy, 24, 345-370.

Tlili, A., Smith, D.C., Beny, J.-M., and Boyer, H. (1989) A Raman microprobe study of natural micas. Mineralogical Magazine, 53, 165-179.

Toby, B.H., and Von Dreele, R.B. (2013) GSAS-II: the genesis of a modern open-source all-purpose crystallography software package. Journal of Applied Crystallography, 46, 544-549.

Trønnes, R.G. (2002) Stability range and decomposition of potassic richterite and phlogopite end members at 5-15 GPa. Mineralogy and Petrology, 74, 129-148.

Tropper, P., Manning, C.E., Essene E.J., and Kao, L.-S. (2000) The compositional variation of synthetic sodium amphiboles at high and ultra-high pressures. Contributions to Mineralogy and Petrology, 139, 146-162.

Welch, M.D., and Graham, C.M. (1992) An experimental study of glaucophanic amphiboles in the system Na_2O-MgO-$A1_2O_3$-SiO_2-SiF_4 (NMASF): some implications for glaucophane stability in natural and synthetic systems at high temperatures and pressures. Contributions to Mineralogy and Petrology, 111, 248-259.

Witte, P. (1975) Synthesis and stability of amphibole phases and anhydrous Na-Mg-silicates in the system Na_2O-MgO-SiO_2-H_2O, the compatibility relationships in the Si-rich part of the quaternary system above 600ºC in the pressure range 1 atm–5kb (H_2O) and their petrological significance]. PhD Thesis, Ruhr-University Bochum, Germany, 256 pp.

Figure captions

Figure 1. Compositions of phases relevant to eckermannite and glaucophane stability at high pressure. Projection from SiO_2 and H_2O onto Na_2O-MgO-Al_2O_3. *ap* = aspidolite, *ek* = eckermannite, *en* = enstatite, *gp* = glaucophane, *jd* = jadeite, *mk* = Mg-katophorite, *ny* = nyboite, *pw* = preiswerkite, *py* = pyrope, *ta* = talc. The experimental bulk composition lies on the intersection of the *ek*-*py* and *ap*-*jd* joins (shown by dashed lines).

Figure 2. **(a)** Secondary-electron image of eckermannite crystals from Experiment 2 (6.2 GPa, 580–670 °C). **(b)** Bright-field HRTEM image of an eckermannite crystal from Experiment 1 (6.2

GPa, 510–620 °C) viewed along *a** and showing (0*k*0) fringes, showing the characteristic amphibole double-chain structure.

Figure 3. Rietveld refinement of eckermannite from Experiment 2. Line markers indicate calculated peak positions. The residual unfitted data are shown below the fitted pattern.

Figure 4. Unpolarised Raman spectrum in the OH-stretching region of eckermannite from Experiment 2.

This is a preprint, the final version is subject to change, of the American Mineralogist (MSA)
Cite as Authors (Year) Title. American Mineralogist, in press.
DOI: https://doi.org/10.2138/am-2018-6399

Howe et al. Figure 1

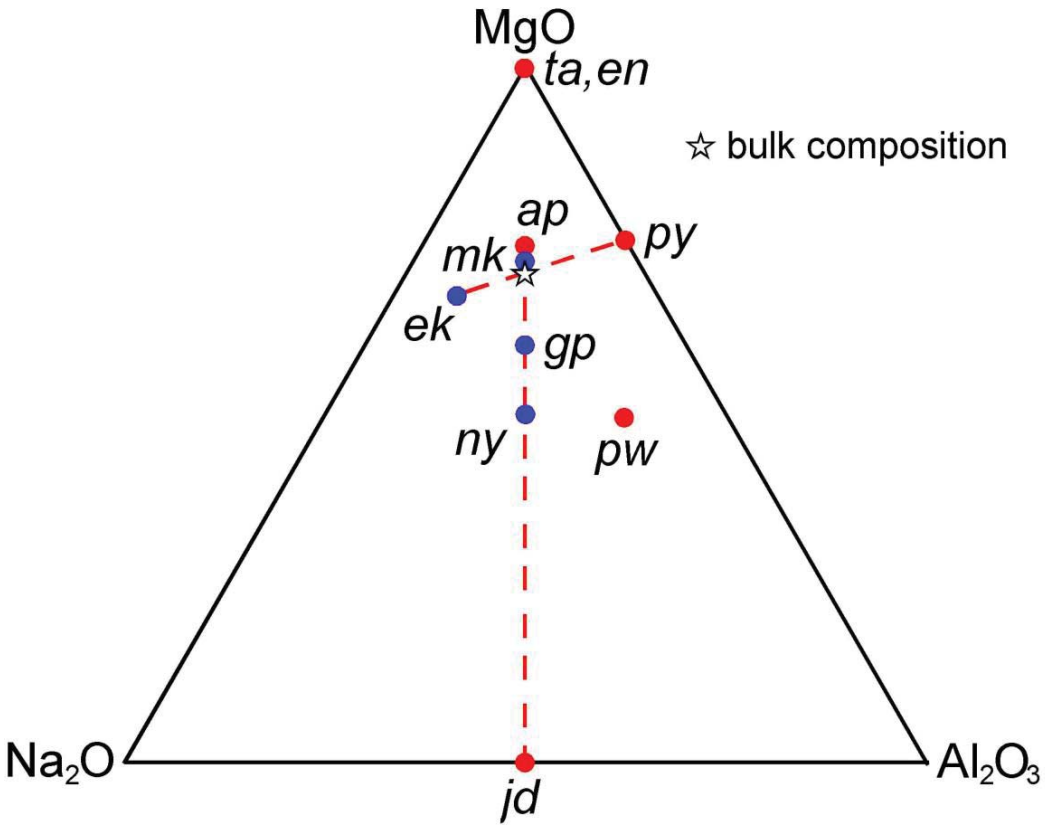

This is a preprint, the final version is subject to change, of the American Mineralogist (MSA)
Cite as Authors (Year) Title. American Mineralogist, in press.
DOI: https://doi.org/10.2138/am-2018-6399

Howe, Pawley, Welch Figure 2

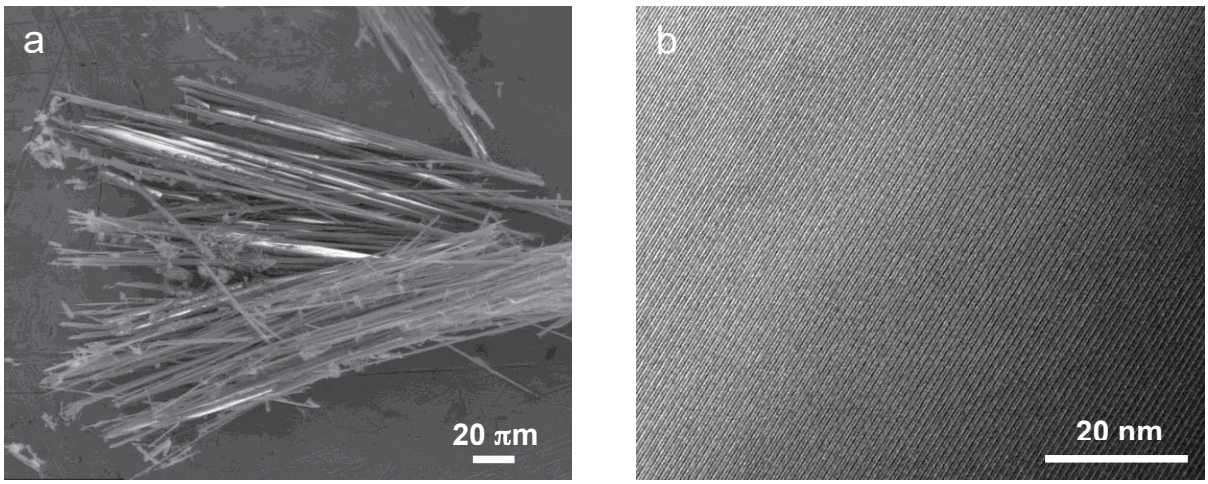

This is a preprint, the final version is subject to change, of the American Mineralogist (MSA)
Cite as Authors (Year) Title. American Mineralogist, in press.
DOI: https://doi.org/10.2138/am-2018-6399

Howe, Pawley, Welch Figure 3

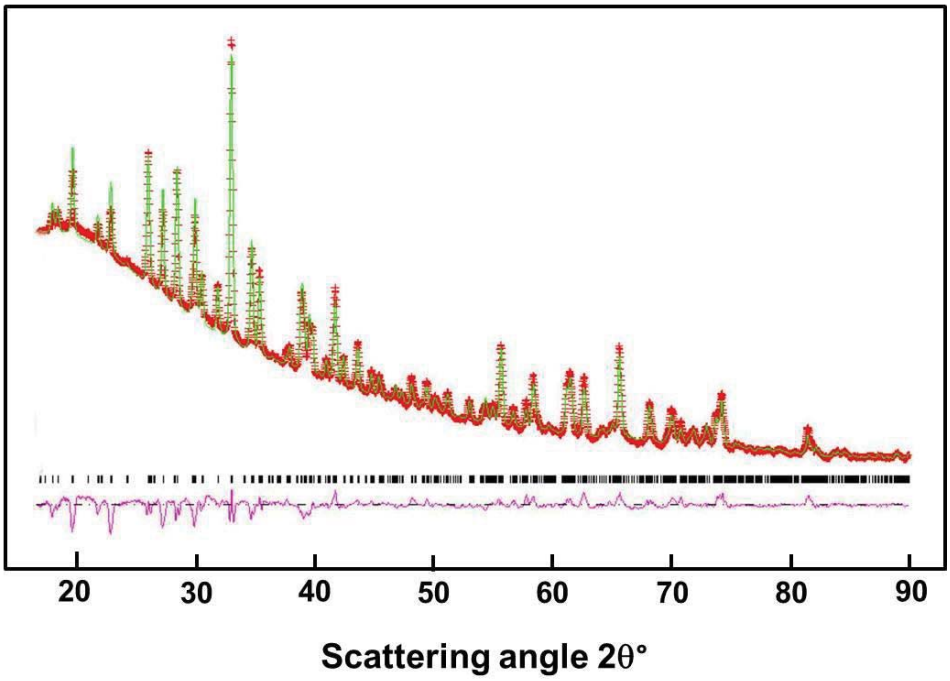

This is a preprint, the final version is subject to change, of the American Mineralogist (MSA)
Cite as Authors (Year) Title. American Mineralogist, in press.
DOI: https://doi.org/10.2138/am-2018-6399

Howe, Pawley, Welch Figure 4